PWM Control of a Buck Converter with an Amorphous Core Coil

José A. Somolinos[1], Rafael Morales[2], Carlos Morón[3] and Alfonso García[3]

[1]ETS de Ingenieros Navales. Universidad Politécnica de Madrid, Arco de la Victoria s/n 28040 Madrid, SPAIN
[2]ETS de Ingenieros Industriales. Universidad de Castilla-La Mancha, Campus Universitario s/n 02071 Albacete, SPAIN
[3]Grupo de Sensores y Actuadores. Avenida de Juan de Herrera s/n 28040 Madrid, SPAIN

Pulse-width modulation is widely used to control electronic converters. One of the most topologies used for high DC voltage/low DC voltage conversion is the Buck converter. It is obtained as a second order system with a LC filter between the switching subsystem and the load. The use of a coil with an amorphous magnetic material core instead of air core lets design converters with smaller size. If high switching frequencies are used for obtaining high quality voltage output, the value of the auto inductance L is reduced throughout the time. Then, robust controllers are needed if the accuracy of the converter response must not be affected by auto inductance and load variations. This paper presents a robust controller for a Buck converter based on a state space feedback control system combined with an additional virtual space variable which minimizes the effects of the inductance and load variations when a not-too-high switching frequency is applied. The system exhibits a null steady-state average error response for the entire range of parameter variations. Simulation results are presented.

***Index Terms*—Buck Converters, Induction aging, PWM control**

I. Introduction

BUCK CONVERTERS are widely used for DC high-voltage/DC low-voltage conversion when high efficiency is required. It consists on a switching system which is controlled by PWM (Pulse Width Modulation) and a L-C network which is coupled with the load [1]. Since the parameter values L, C, and load R_L define the system dynamics, variations of any of them modify the load voltage which is the variable controlled by the converter. Variations over R_L are defined by the relation between the output voltage and the current to be drawn from the converter. The capacity C is not expected to vary throughout the time and the magnetic induction L is affected by errors on the nominal value when an amorphous core coil is used. These magnetic induction properties could shift thoroughout the time due to multitude of causes. These variations may be caused by changes in the coil specifications and/or changes in the core magnetic material properties. These changes in the coil properties may happen for different reasons: variations in the packing factor of coils are usually caused by quickly changes in temperature (heating) that may be permanent or not. Short circuits between contiguous turns of the coil could appear because of any kind of loss of isolation. This may be caused by overheating or abrasion. Depending on the number of turn affected and the total turns, inductance variations could be significant.

Additionally, in magnetic core coils, it is well known that the induction value decreases throughout the time because of changes in the core magnetic properties such as anisotropy direction or coercive field. These variations are produced by material heating or heating-cooling cycles that are similar to undesirables annealing treatments. Different authors have shown that the coercive field increases with annealing temperature and time due to the growth of the magnetic material grain size or the magnetic anisotropy direction dispersion [2]-[5]. At the same time, it is well known that the magnetic losses (and therefore the activation energy in magnetic cores) increase with the magnetic field frequency [6],[7]. Finally, if temperature and/or ambient conditions enables it, chemical changes in the core may happen [8],[9] which are clearly associated with heating. Thus, the higher frequency of the current applied to the induction is, the most significant aging parameter which affects the induction magnetic cores. This aging effect is translated into a time decreasing induction value.

Traditional control systems for L-C circuits use a linear time invariant model with small parameter changes. They exhibit accurate responses when modulation frequencies are much higher than the frequency of the system. However, a non-nominal design of the control system is required when not too high modulation frequency is chosen (in order to limit the heating of the switching elements) and the L-C network parameters cannot be considered as constant.

This paper presents a new state-space control system which is robust against changes in the inductance L and large changes in the load R_L (voltage/current). If a second order state-space feedback is used, a null steady-state average error is obtained only for changes in the inductance L. However, if large changes in R_L are produced too, steady-state errors in the output voltage appears and the addition of a virtual state variable that combined with a state-space feedback (producing a third order system) allow to obtain accurate responses when variations in L and R_L are produced in the system.

Manuscript received January 1, 2008 (date on which paper was submitted for review). Corresponding author: J.A. Somolinos (e-mail: joseandres.somolinos@upm.es).
Digital Object Identifier inserted by IEEE

The paper is organized as follows: Section II describes the dynamic model. Section III develops the proposed control system. Section IV shows the steady-state behavior of the converter. Section V presents several simulation results and Section VI states some conclusions.

II. Dynamic Modeling of the Converter

Figure 1 illustrates a typical Buck converter with a switch implemented as a N depletion mode MOSFET transistor.

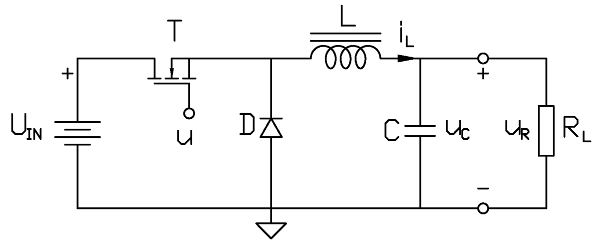

Fig 1. Buck Converter

If current over the coil $i_L(t)$ and voltage of the capacitor $u_C(t)$ are used as state variables $x = (i_L \quad u_C)^T$, the model of the converter is:

$$\begin{cases} \dot{x}(t) = A_C \cdot x(t) + B_C \cdot u(t) \\ y(t) = C_C \cdot x(t) \end{cases} \tag{1}$$

With matrices A_C, B_C and C_C respectively being:

$$A_C = \begin{pmatrix} 0 & -1/L \\ 1/C & -1/R_L C \end{pmatrix}, \quad B_C = \begin{pmatrix} 1/L \\ 0 \end{pmatrix}, \quad C_C = \begin{pmatrix} 0 & 1 \end{pmatrix} \tag{2}$$

Where *u(t)* denotes the system input, *y(t)* denotes the converter output $y(t) = u_C(t) = u_R(t)$ and R_L denotes the load.

Nominal parameters values are L_0 = 10 mH, C = 25 μF and R_{L0} = 10 Ω with input U_{IN} = 100 V and a desired output of U_R = 50 V. Under these nominal values the system exhibits a critically damped dynamics with a frequency ω_0 = 2000 rad/s which is taken from:

$$\frac{1}{L_0 C} = \omega_0^2 = \frac{1}{(2 \cdot R_{L0} C)^2} \tag{3}$$

If it is represented by its input-output relation, a transfer function between U and Y is obtained.

$$\frac{Y(s)}{U(s)} = G_C(s) = \frac{1/L_0 C}{s^2 + 1/R_{L0} C \cdot s + 1/L_0 C} \tag{4}$$

Being *s* the Laplace complex argument. From this representation and by applying the final value theorem, steady –state responses of system (2) with step inputs are given by:

$$y_S = y(t = \infty) = Y(s = 0) = U \cdot G_C(0) \tag{5}$$

The switching frequency is f_S = 2 kHz. The relation between the switching frequency and the nominal system frequency f_0 becomes 6.28 which is close to the lower limit given in [10]:

$$5 \leq \frac{f_S}{f_0} \leq 40 \tag{6}$$

The variation ranges considered for the coil core and the load are the following:

$$\begin{gathered} 0.8 \cdot L_0 \leq L \leq L_0 \\ R_{L0} \leq R_L \leq 10 \cdot R_{L0} \end{gathered} \tag{7}$$

Moreover when an ON-OFF PWM controller is used, input is of the form:

$$u(t) = \begin{cases} 0 & \mathit{for} \quad Tk \leq t < T(k+1-d(k)) \\ U_{IN} & \mathit{for} \quad T(k+1-d(k)) \leq t < T(k+1) \end{cases} \tag{8}$$

Being $T = (f_S)^{-1}$, k an integer, and $0 \leq d(k) \leq 1$ the duty ratio (relative pulse width). Steady-state average responses (denoted with $\__S$) for a given average d_S then become:

$$\bar{y}_S = \bar{y}_S(t = \infty) = U_{IN} \cdot G_C(0) \cdot (0 + 1 \cdot d_S) \tag{9}$$

Which can be normalized for $d_S > 0$ and it results:

$$\bar{y}_{S\_UNIT}(t = \infty) = \frac{U_{IN} \cdot G_C(0) \cdot (0 + 1 \cdot d_S)}{d_S} \tag{10}$$

Responses from both equations (5) and (9) coincide if $U = U_{IN}/d_S$ or system (2) includes this scale factor d_S into matrix B_C (which is similar to scale the numerator of $G_C(s)$). These average responses do not depend on modulation frequency although their ripple amplitude will be smaller the higher this frequency. However switching components (transistor T and diode D) will increase their heating which is an undesired effect.

III. Control System

Controllability matrix (See[11]) of the given system results:

$$Q_C = \begin{pmatrix} B_C & B_C \cdot A_C \end{pmatrix} = \begin{pmatrix} 1/L & 0 \\ 0 & 1/LC \end{pmatrix} \tag{11}$$

With *range(Q$_C$)* = 2 for all values of L, C ≠∝. Then the system results fully controllable.

If *r* denotes a reference signal, the control input *u* is composed by a combination of a feed-fordward term and a state-space feedback term. It is defined as:

$$u = K_{W0} \cdot r + K_{F0} \cdot x \tag{12}$$

Figure 2 shows a simple state-space control system diagram.

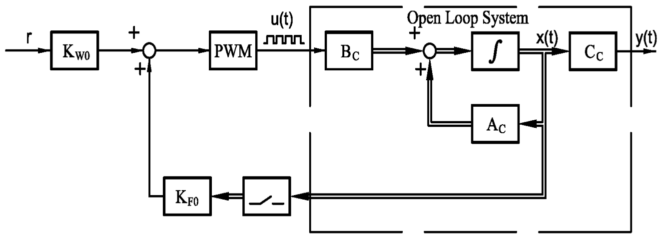

Figure 2. State-space feedback

After choosing the desired eigenvalues of the controlled system (roots of the denominator of the closed loop transfer function), the feed-forward term K_{W0} and the gain matrix K_{F0} are calculated for nominal values. As example, if desired eigenvalues are $\sigma_{10} = \sigma_{20} - 5/R_{L0}C$, they correspond with a desirable characteristic polynomial of the form:

$$\phi_{Des}(\lambda) = \lambda^2 + \left(\frac{10}{R_{L0} C}\right)\lambda + \frac{25}{R_{L0}^2 C^2} \tag{13}$$

then, the gain matrix K_{F0} and K_{W0} are easily obtained as:

$$K_{F0} = \begin{pmatrix} \dfrac{-9L_0}{R_{L0}C} & 1-\dfrac{16L_0}{R_{L0}^2C} \end{pmatrix}, \quad K_{W0} = 100 \tag{14}$$

If non-nominal conditions (variations in L and R_L) are considered, the characteristic polynomial of the controlled system $\phi(\lambda)$ becomes:

$$\lambda^2 + \left(\frac{9L_0R_L}{LR_{L0}} + 1\right)\frac{1}{R_LC}\lambda + \left(\frac{9L_0R_L}{LR_{L0}} + \frac{16L_0R_L^2}{LR_{L0}^2}\right)\frac{1}{R_L^2C^2} \tag{15}$$

Also, in order to evaluate the steady-state system response, the relative average error is defined as $\varepsilon_r = (\bar{r}_S - \bar{y}_S)/\bar{r}_S$ where $\bar{r}_S$ denotes the average reference value.

According to equation (15) if $R_L = R_{L0}$ remains constant and only variations in L are considered, the eigenvalues of the controlled system $\sigma_{1R_0}, \sigma_{2R_0}$ are real and vary from the nominal ones while relative average error (from equations (12),(15) and the last term of denominator from eq.(4)) is:

$$\varepsilon_{rR_{L0}} = 1 - \frac{K_{W0}\cdot 1/LC}{\dfrac{25\cdot L_0}{L}\ 1/R_{L0}^2C^2} = 1 - 1 = 0 \tag{16}$$

Which is not L-dependant. However, if non nominal values of R_L are considered too, new eigenvalues become from –23.5 to -5 $(R_{L0}C\cdot\sigma_1)$ and $(R_{L0}C\cdot\sigma_2)$ from –90.3 to –5 which imply larger system frequencies than f_S and the controlled system will not provide good responses. Under these conditions it exhibits a minimum/maximum average relative errors which are given by:

$$\varepsilon_r = 1 - \frac{25}{9\cdot R_{L0}/R_L + 16} = \begin{cases} 0 & if \quad R_L = R_{L0} \\ -0.479 & if \quad R_L = 10R_{L0} \end{cases} \tag{17}$$

To cancel these errors, a new state variable is created:

$$\dot{x}_\varepsilon = r - y = r - C_C\cdot x \tag{18}$$

and the control signal *u* (See figure 3) is now computed as:

$$u = K_{\varepsilon 0}\cdot x_\varepsilon + K_{F\varepsilon 0}\cdot x \tag{19}$$

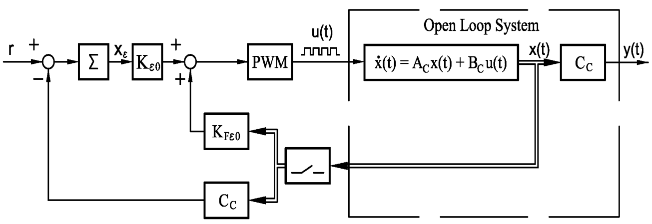

Figure 3. State-space feedback with a virtual state variable

The new expanded system is then written as:

$$\begin{pmatrix}\dot{x}_\varepsilon(t)\\ \dot{x}(t)\end{pmatrix} = \begin{pmatrix}0 & -C_C\\ 0 & A_C\end{pmatrix}\cdot\begin{pmatrix}x_\varepsilon(t)\\ x(t)\end{pmatrix} + \begin{pmatrix}0\\ B_C\end{pmatrix}\cdot u + \begin{pmatrix}1\\ 0\end{pmatrix}\cdot r \tag{20}$$

and using the control law given by equation (19), the controlled system (with $K_{F\varepsilon 0} = (k_{1\varepsilon} \quad k_{2\varepsilon})$) becomes:

$$\begin{cases}\dot{\hat{x}}(t) = \hat{A}_C\cdot x(t) + \hat{B}_C\cdot r(t)\\ y(t) = \hat{C}_C\cdot\hat{x}(t)\end{cases} \tag{21}$$

$$\hat{A}_C = \begin{pmatrix} 0 & 0 & -1\\ K_{0\varepsilon}/L & k_{1\varepsilon}/L & (k_{2\varepsilon}-1)/L\\ 0 & 1/C & -1/R_L\cdot C\end{pmatrix} \quad B_C = \begin{pmatrix}1\\0\end{pmatrix} \tag{22}$$

$$\hat{C}_C = \begin{pmatrix}0 & 0 & 1\end{pmatrix}$$

By assigning its characteristic polynomial $\det\left(\hat{A}_C - \hat{\lambda}\cdot I^{3x3}\right)$ to the polynomial from the desired eigenvalues $(R_{L0}C\cdot\hat{\sigma}_1 = R_{L0}C\cdot\hat{\sigma}_2 = -5$ and $R_{L0}C\cdot\hat{\sigma}_3 = -1)$ which is:

$$\phi_{Des}(\hat{\lambda}) = \hat{\lambda}^3 + \frac{11}{R_{L0}C}\cdot\hat{\lambda}^2 + \frac{45}{R_{L0}^2C^2}\cdot\hat{\lambda} + \frac{25}{R_{L0}^3\cdot C^3} \tag{23}$$

all gains to the control law from equation (19) are obtained:

$$K_{\varepsilon 0} = \frac{100}{R_{L0}C} \quad K_{F\varepsilon 0} = \begin{pmatrix} -\dfrac{10L_0}{R_{L0}C} & -134 + \dfrac{10}{R_{L0}^2C}\end{pmatrix} \tag{24}$$

IV. Steady State Behavior

In this section is analyzed the relative average errors when control signal is given by eq.(19). The gains are obtained from equation (24) and non-nominal conditions have been included. The characteristic polynomial of the matrix $\hat{A}_C$ becomes:

$$\begin{aligned}\phi(\hat{\lambda}) = \hat{\lambda}^3 &+ \left(\frac{1}{R_L} + \frac{10\cdot L_0}{LR_{L0}}\right)\frac{1}{C}\hat{\lambda}^2 + \\ &+ \left(135 - \frac{10}{R_{L0}^2C}\cdot\left(1 - \frac{R_{L0}}{R_L}\right)\right)\frac{1}{LC}\hat{\lambda} + \frac{100}{R_{L0}LC^2}\end{aligned} \tag{25}$$

where it can be observed that it is different from the desired $\phi_{Des}(\hat{\lambda})$. From the new last term of this polynomial, the new relative average errors are then cancelled according to:

$$\varepsilon_{r\varepsilon} = 1 - \frac{K_{\varepsilon 0}\cdot 1/LC}{\dfrac{100}{R_{L0}LC^2}} = 1 - 1 = 0 \tag{26}$$

for all the values of L and R_L in the range defined in (7).

V. Simulation Results

Different simulations have been carried out using the linearization technique from [12] with f_s = 2 kHz and varying the parameters L and R_L. Figure 4 depicts some output responses when the control law (12) is used for controlling the system with different values of L and R_L. A step signal is used as reference with 1 ms of rise time from 0 to 50V at t_1=1 ms.

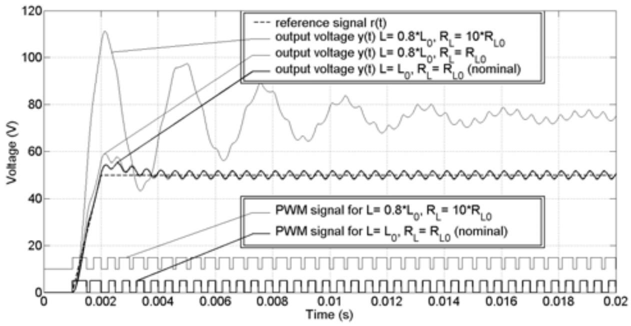

Fig. 4. Time response of the converter

It can be observed how the output has reduced its damping and it cannot reach the reference in the so-called worst case ($R_L = 10.R_{L0}$ and $L = 0.8.L_0$). The steady-state average ouput is 74.72V under this condition while the reference is 50V. Both values let obtain a relative average error $\varepsilon_r = (50 - 74.72)/50 = -0.494$ which is in accordance with equation (17). At the bottom of figure 4 is plotted the PWM controller responses for both the nominal and worst cases.

Figure 5 illustrates the converter responses when the proposed control law (19)-(24) is used for controlling the voltage outputs with the same reference signal. PWM responses for nominal and worst cases are plotted too.

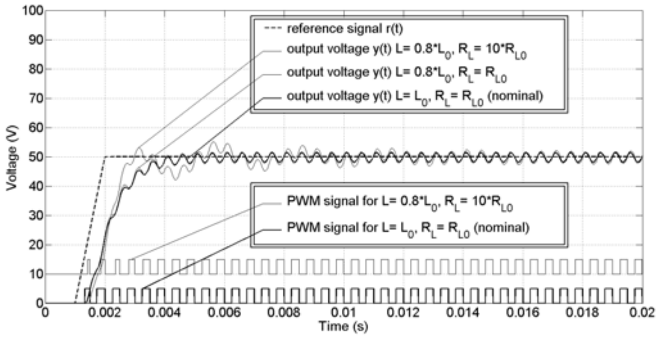

Fig. 5. Time response of the converter

The controlled system exhibits slower responses than the previous. This is because the dominant eigenvalue desired $\hat{\sigma}_3$ has been chosen of a value smaller than σ_{10}, σ_{20}. Thus the steady-state average errors are cancelled for every value of L and R_L (even in the worst case) which is in accordance with equation (26).

Finally, in order to show the valuable results of the controller proposed, two output responses from two sets of parameters have been plotted in figure 6: the nominal one and other with the worst case ($L=0.8.L_0$ and $R_L=10.R_{L0}$) when a new reference signal is applied. It switchs at t_1=1 ms from 0V to 75V then it drops to 25V at t_2=25 ms and finally, it reaches the nominal 50V at t_3=50 ms. All the transitions are generated with rise/fall times of 1ms.

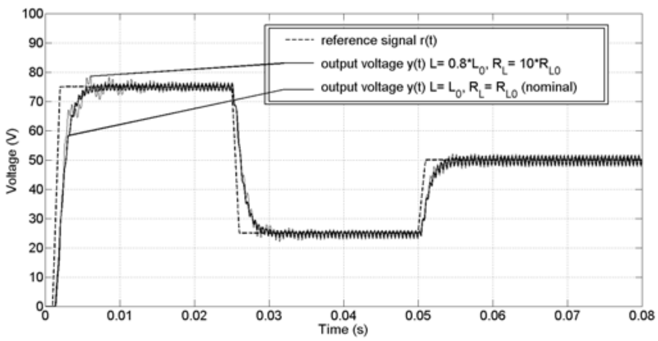

Figure 6.- Output voltage with variable reference.

The relative average errors are cancelled for all the parameter values while the ripple has not increased significantly in either both cases (Modulation frequency is the same).

VI. Conclusions

A robust control of a Buck converter with an amorphous core coil and variable load (voltage and current relation) has been presented. It is controlled via PWM under relative small modulation frequencies. State-space controllers which use coil current and capacitor voltage as state variables can be used for controlling this kind of converters with fast responses and null steady-state average errors; even in the case that the coil inductance decreases its value throughout the time. However, if a non-nominal load is used (which implies that current drawn from the converter can be very different from the nominal) the controller response may not operate properly. An additional virtual state variable that increases the order of the system combined with a state-space feedback let control the converter over the entire range of parameters including a decrease in L due to aging and a high increment of the value of R_L. The well known correspondence between the responses of real electronic circuits and simulation results for this kind of systems allow us to test the proposed method and validate the control proposed.

Acknowledgment

This work was supported in part by the Spanish Ministerio de Ciencia e Innovación under Grant DPI2011-24113.

References

[1] N. Mohan, Tore M. Undeland and William P. Robbins. *Power Electronics: Converters, Applications, and Design*. John Wiley & Sons.

[2] R.A. Renzetti, H.R.Z. Sandim, M.J.R. Sandim, A.D. Santos, A. Möslang and D. Raabe, "Annealing effects on microstructure and coercive field of ferritic–martensitic ODS Eurofer steel", *Materials Science and Engineering A*, 2011 vol. 528, Is. 3 pp. 1442-1447.

[3] M. J. Sablik, D. Stegemann, and A. Krys "Modeling grain size and dislocation density effects on harmonics of the magnetic induction" *Journal of Applied Physics*, 2001 Vol. 89, pp 7254–7256.

[4] M.F. de Campos, T. Yonamine, M. Fukuhara, F.J.G. Landgraf, C.A. Achete, F.P. Missell, "Effect of Frequency on the Iron Losses of 0.5% and 1.5% Si Nonoriented Electrical Steels", *IEEE Transactions on Magnetics*, 2006 Vol. 42, pp. 2812–2814.

[5] D. Bisero, E. Angeli, F. Spizzo, P. Vavassori, F. Ronconi,"Coercive field vs. temperature in Fe/Ag nanogranular films", *Journal of Magnetism and Magnetic Materials*, 2003 Vol. 262, pp. 116-119.

[6] A. Lakshman, P.S.V. Subba Rao and K.H. Rao, "Frequency dependence of initial permeability and magnetic loss factor of In3+ and Cr3+ substituted Mg–Mn ferrites", *Journal of Magnetism and Magnetic Materials*, 2004 Volume 283, Issues 2-3, pp. 329-334.

[7] H. G. Brachtendorf and R. Laur, "Modeling of hysteresis in magnetic cores with frequency-dependent losses", *Journal of Magnetism and Magnetic Materials*, 1998 Volume 183, pp. 305-312.

[8] *G.E. Fish, "Stability of magnetic properties of metallic glasses",* IEEE Transactions on Magnetics, *1985 MAG-21 (5), pp. 1996-2001.*

[9] W. McKinnon, J.W. Choung, Z. Xu and J.A. Finch, "Magnetic Seed in Ambient Temperature Ferrite Process Applied to Acid Mine Drainage Treatment", *Environ. Science & Technology*, 2000, 34, pp. 2576-2581.

[10] S. Jung and Y. Tzou, "Discrete sliding-mode control of a PWM inverter for sinusoidal output wave form systhesis with optimal sliding curve" *IEEE Trans. Power Electron., 1996,* Vol. 11, pp. 567-577.

[11] K. Ogata "Modern Control Engineering" 5th Edition. Pearson. 2010

[12] Ignacio Nuez and Vicente Feliu, "On the Pulse-Width Modulation Control of L-C Filtres" IEEE Trans. On Circuits and Systems Part I, 2000, Vol. 47, No 3, pp 338-349